11th International Symposium on Turbulence and Shear Flow Phenomena (TSFP11)
Southampton, UK, July 30 to August 2, 2019

SPATIO-TEMPORAL STRUCTURE OF NATURAL CONVECTION BOUNDARY LAYER ALONG A HORIZONTAL HEATED ROUND PLATE

Yasuo Hattori

Civil Engineering Research Laboratory
Central Research Institute of Electric Power Industry
1646 Abiko, Abiko-shi, Chiba-ken, 270-1194, Japan
yhattori@criepi.denken.or.jp

Hitoshi Suto

Civil Engineering Research Laboratory
Central Research Institute of Electric Power Industry
1646 Abiko, Abiko-shi, Chiba-ken, 270-1194, Japan
suto@criepi.denken.or.jp

Keisuke Nakao

Civil Engineering Research Laboratory
Central Research Institute of Electric Power Industry
1646 Abiko, Abiko-shi, Chiba-ken, 270-1194, Japan
nakao@criepi.denken.or.jp

Yuzuru Eguchi

Civil Engineering Research Laboratory
Central Research Institute of Electric Power Industry
1646 Abiko, Abiko-shi, Chiba-ken, 270-1194, Japan
eguchi@criepi.denken.or.jp

ABSTRACT

A development processes, including turbulence transitions, of a natural-convection boundary layer in air along an isothermally heated round plate was experimentally investigated, especially paying attention to the interaction with organized motions in a buoyant plume above the boundary layer. The heated round plate, the diameter of which was 300 mm, was horizontally placed in a test section of chamber. The upper-surface temperature was kept at 473 K, and thus the values of dimensionless temperature difference and Rayleigh number based on the diameter were about 0.6 and 3.0×10^8, respectively, which correspond to those for a turbulent boundary layer above the heated plate with non-Boussinesq effects. The turbulence statistics of temperature fluctuations in the boundary layer, including near the heated surface, were measured by a cold wire, and 2-components velocity vectors in a vertical plane of the boundary layer and of the buoyant plume were measured by using a PIV measurement. The dynamic ranges of PIV measurement were improved by a two-camera PIV technique, and the accuracy of PIV measurement was verified through the comparison with a hot-wire measurement. These measurements and organized motions extracted with a proper orthogonal decomposition clearly showed the coexistence of the development of boundary layer, which yields turbulence transitions with vortices intermittently moved toward the centre of the plate. Such a coexistence gives the unsteady evolution of the boundary layer with wavy motions, which were observed by the snapshots of reconstructed velocity vectors with the proper orthogonal decomposition.

INTRODUCTION

Accurate descriptions of heat-transfer characteristics in a turbulent natural-convection boundary layer along upward-facing finite-sized and highly-heated source in air are practical interest in engineering applications, such as heat removal design for nuclear-power plants and fireproof design for buildings. Many empirical formulas for the heat transfer rate, which is one of the most important thermal property for engineering applications, have been already reported, but there exists considerable scattering of calculations among them (Khalifa 2001). Also, studies on the turbulence characteristics near a heat source, which are closely related to the heat transfer from a heat source, are startlingly few even for simple objects (Theerthan and Arakeri, 1998).

The insufficiency of a understanding for heat-transfer and turbulence characteristics of the boundary layer might be due to the difficulty in reducing uncertainty of obtaining turbulence statistics near a heat source with experiments and numerical simulations. The experiments have some difficulty of reliable turbulence measurements for low-speed flows with large fluctuations in velocity and temperature (Hattori et al., 2006), and the numerical simulations have tasks on improvement of turbulence models to precisely represent small eddy structures, which appear near a heat source (Pham et al., 2007). Also, preservation of steady conditions should be also assured in the experiments and numerical simulations (Plourde et al., 2008; Hu et al. 2015).

On the other hand, some numerical and experimental studies have revealed an interaction between vortex rings near a heat source and a development process of thermal plume (Brown et al. 2006; Pham et al., 2007; Plourde et al., 2008). Such the interaction between the organized motions and the flow fields near the edge of the heated surface implies the dynamics of the buoyant plume with large-scale fluid motions affect the development processes of the boundary layer along a heated surface and the heat transfer processes of the boundary layer. Kitamura and Kimura (1995) and Kitamura and Kimura (2007) also suggested that changes in the heat transfer characteristics with the coherence structures generated in the development of the boundary layer above a locally heated horizontal surface.

In this study, a natural-convection boundary layer with transition to turbulence in air near the upper surface of a heated round plate in air is experimentally investigated, especially paying attention to the interaction with organized motions in a buoyant plume above the boundary layer. The boundary layer is generated by an isothermally heated round plate, the surface temperature and diameter of which are 473 K and 300 mm, respectively. The turbulence statistics of temperature fluctuations in the boundary layer, including near the heated surface, are measured by a cold wire, and 2-components velocity vectors in a vertical plane of the boundary layer and of the buoyant plume are measured by using a PIV measurement. With these measurements and organized motions extracted with a proper orthogonal decomposition which is a tool for

coherence structures in the buoyant flows (Watanabe et al. 2015) turbulence statistics in the thermal field of the boundary layer including in the vicinity of the heated surface and also the dynamics of fluid field of the development of the boundary layer and the buoyant plume are discussed in details.

EXPERIMENTAL SETUP

Experimental Apparatus

A schematic drawing of experimental apparatus is shown in Fig. 1. A round heated plate, the diameter of which, D, was 300 mm, was horizontally mounted on the bottom wall in a test section of chamber.

This chamber was used to reduce disturbances included in ambient fluid. Working fluid is air. The dimension of chamber was 1,600 × 1,600 mm^2 (= 5.3D × 5.3D) in area and 1,500 mm (= 5D) in height. The whole chamber was coated with a thick layer of heat insulating material and surrounded by damping screens. The ventilation of chamber was carried out with a small flow rate (about 0.03 m^{3}s^{-1}) to prevent the generation of thermal stratification near the heated plate.

The heated round plate comprised an aluminium disk (20 mm in thickness), casting heaters, thermocouples and control systems. The upper surface of aluminium disk was polished to a mirror finish to minimize the heat loss by radiation. The casting heaters, the total output of which was 3 kW, were attached to the backside of the disk. The upper-surface temperature of disk was monitored by K-type sheath thermocouples. Based on the output from thermocouples, the electric supply for each heater was controlled with digital indicating controllers and thirstier regulators, and the upper-surface temperature was kept steady and uniform during experiments.

The coordinate system used in the present study is also shown in Fig. 1. The origin of the co-ordinate is located at the centre of the upper surface of the heated round plate; x and z are the horizontal distance from the centre and the vertical distance from the heated surface, respectively. The horizontal distance from the edge of the heated plate is refer to x' ($x' = D/2 - x$).

Temperature and Velocity Measurement

Two kinds of measurements were carried out: one was a cold-wire measurement to obtain turbulence statistics of temperature fluctuation, and the other was a PIV measurement examine the dynamics of organized motions due to the development of the boundary layer and buoyant plume.

A cold wire was used to measure instantaneous temperature. It was 3.1 μm diameter tungsten, and the shape and dimensions of the probe were set so as to minimize measurement errors. The sensitive length was 4 mm with the aspect ratio of 1290, which is fully large to eliminate the decay of measured temperature fluctuations in the low frequency regions with the heat conduction to the prong (Tsuji et al. 1992). The configuration of the probe was for boundary layer flows to measure instantaneous temperatures even in the vicinity of the heated surface. The sampling frequency and sampling time were 1,000Hz and 260s, respectively for each measuring point.

The 2-components velocity vectors in a vertical (x-z) plane along a centre line of a plume were measured with a PIV technique. A two-camera PIV technique (Hattori et al. 2018)

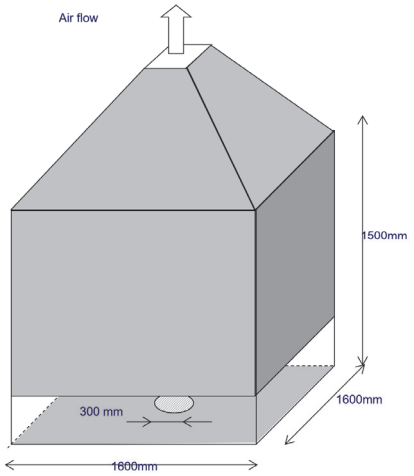

Figure 1. Schematic drawing of experimental apparatus with coordinate system used in present study.

was used to ensure spatial fine resolutions for capturing turbulence vortices as well as a large visualized area for observing development process of the boundary layer. Particle-containing flow images were captured by two CCD cameras (2 × [2,048 × 2,048 pixels]). The cameras had the same specifications. On the other hand, one was attached a F200 micro Nikkor lens and the other was attached a F105 micro Nikkor lens. The distances between the lens and the object plane was approximately 800 mm, and the physical size of the measuring areas were 60 × 60 mm^2 (= 0.2D × 0.2D) for F200 lens and 120 × 120 mm^2 (= 0.4D × 0.4D) for F105 lens. Visualized image data was stored into a memory of camera at about 7 frames per second. Velocity vectors were calculated by using a cross-correlation method. The interrogation windows size and the overlap ratio were 16 × 16 pixels and 50%, respectively, and the 65,536 velocity vectors were obtained in each pair of images. A sub-pixel algorithm assuming a Gaussian profile for the spatial correlation was also applied to improve the dynamic spatial range of velocity vectors. After calculating velocity vectors, incorrect velocity vectors were removed with a median filter, and empty data grids were filled with interpolated velocity vectors. The sampling frequency and sampling time were 7Hz and 420s, respectively.

Experimental Condition and Procedure

The experiments were carried out under the condition of constant and uniform upper-surface temperature Tw of 473 K. The ambient fluid temperature Ta was somewhat different for each experiment, in the range of 295 – 297 K. Thus, the dimensionless temperature difference $\beta\Delta Tw$ ($\Delta Tw = Tw - Ta$) was about 0.6, where coefficient of volumetric expansion β is $1/Ta$, implying that non-Boussinesq effects may appear (Ai et al. 2006). As the temperature difference between the upper surface and ambient increases, the variable property effects on the normalization of experimental data becomes significant, so that some reference temperature methods have been recommended. The value of Rayleigh number, based on the diameter of heated surface, Ra_D ($Ra_D = Gr_D \cdot Pr$; $Gr_D = g\beta\Delta TwD^3/\nu^2$, where $Pr = \nu/\alpha$, g, ν and α are gravity

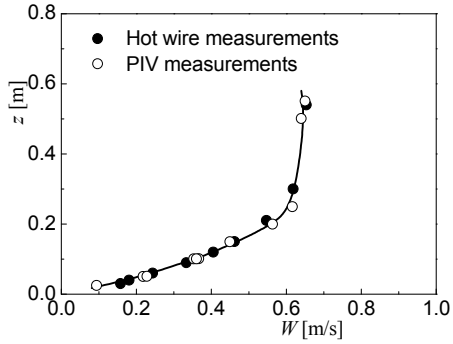

(a) mean value of vertical velocity W

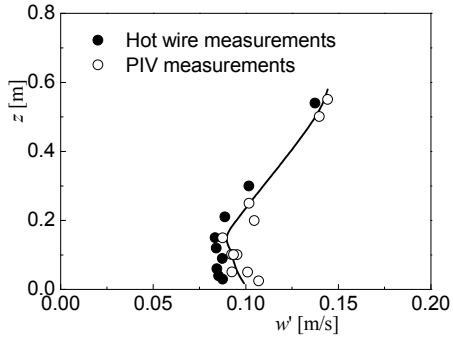

(b) r.m.s. values of fluctuating vertical velocity w'

Figure 2. Comparison of vertical profiles of turbulence statistics with hot wire measurements.

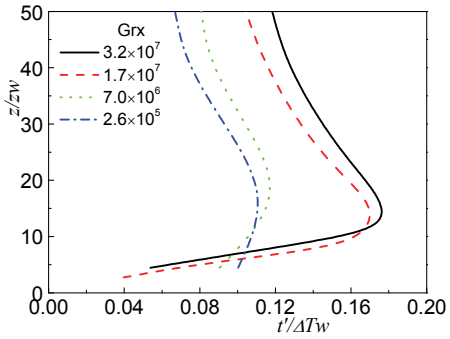

Figure 3. Vertical profiles of r.m.s. value of temperature fluctuation.

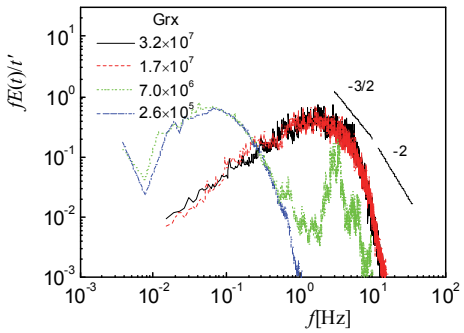

Figure 4. Power spectra of temperature fluctuation near heated surface.

acceleration, kinematic viscosity and thermal diffusivity, respectively) was 7.0×10^8 with the physical properties at the ambient temperature, and 3.0×10^8, with the properties at the film temperature except for β, which has been widely used for turbulent natural convection boundary layer flow along a vertical heated plate (Hattori et al. 2006). These values, regardless of reference temperature, correspond to that for turbulent boundary layer above a heated plate (Kitamura and Kimura 1995, Theerthan and Arakeri 1998, Kitamura and Kimura 2007).

RESULTS

Preliminary Experiment

In the preliminary experiments, we confirmed that flow and thermal fields in the test section and verified the accuracy of these measurements for low-speed flow with large fluctuations in flow- and thermal-fields through the comparison with a hot-wire measurement. Figure 2 shows the comparison of vertical profiles of time averaged and r.m.s. values of vertical (upward) velocities, W and w', along the centre axis of the plume ($x = 0$, above the centre of the heated surface). PIV measurements agree with hot-wire measurements even for the r.m.s. values in the vicinity of the heated surface, where the upward flows are very weak (the time averaged values of upward velocity become almost zero). Note that, we have confirmed reproducibility of the outline of flow pattern (the distribution of W in the boundary layer and the plume) in our experiments, and also the sampling time and the number of data for the temperature measurement were sufficient to reach the reproducibility of experiments, that is, the turbulence statistics, including higher-order moments, do not change significantly with the increase in the sampling time and the data size.

Statistics of Temperature Fluctuations

The vertical profiles of intensity of temperature fluctuations, t', at local Grashof number of $Grx' = 2.6 \times 10^5 - 3.2 \times 10^7$ ($x'/D = 0.1 - 0.5$) are shown in Fig. 3. The profiles are normalized with Townsend's (molecular) characteristics scales (Adrian 1996, Theerthan and Arakeri, 1998): $zw\ [= (\nu\alpha)^{1/2}/Uw$, where $Uw = g\beta\Delta Tw(\nu\alpha)^{1/6}] = 4.9\times10^{-4}$ m. The significant change in the vertical profile occurs at $Grx' = 7.0 \times 10^6 - 1.7 \times 10^7$, i.e., the differences of the profiles between at $Grx' = 2.6 \times 10^5$ and 7.0×10^6 and also between at $Grx' = 1.7 \times 10^7$ and at 3.2×10^7 are quite small; the intensities of temperature fluctuations at $Grx' = 1.7 \times 10^7$ and 3.2×10^7 are large compared with those at $Grx' = 2.6 \times 10^5$ and 7.0×10^6. They also suggest the existence of the similarity of normalized profiles before and after the change in the profiles, while some Grashof number effects are observed, which give slight increases in the intensities with Grx'. The normalized profiles at $Grx' = 1.7 \times 10^7$ and 3.2×10^7 agree with those of Rayleigh-Benard convection under turbulence conditions (Theerthan and Arakeri, 1998); the maximum r.m.s. values and the values of z which give the maximum r.m.s. are roughly 0.16 – 0.2 and 10 – 20.

Power spectra of temperature fluctuations, $E(t)$, near the heated surface (at $z/zw \cong 10$) for $Grx' = 2.6 \times 10^5 - 3.2 \times 10^7$ are shown in Fig. 4. The power spectra are normalized with frequency, f, and intensities of temperature fluctuations, t', to

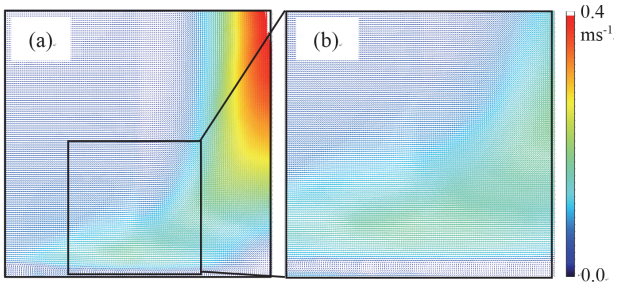

Figure 5. Vectors and contours of time averaged velocity field measured with a F105 (a) and F200 (b) lenses.

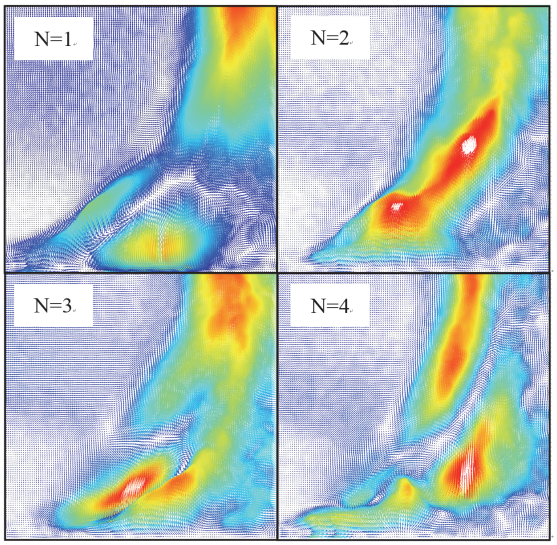

Figure 6. Flow pattern of dominant fluid motions with a F105 lens observed by proper orthogonal decomposition.

clearly grasp the dominant time scale of temperature fluctuation. The frequency, at which power spectrum shows a peak, changes with Grx'. Its frequency at Grx' = 2.6 × 10^5 is about 10^{-1} Hz, and shifts toward higher region with Grx'. Spectrum at Grx' = 7.0 × 10^6 also shows the large contributions at $f \cong 10^{-1}$ Hz to the fluctuations but also has the second peak at $f \cong 10^0$ Hz. Spectra at Grx' = 1.7 × 10^7 and 3.2 × 10^7 takes maximum value at $f \cong 10^0$ Hz. There spectra present rapid decay in the frequency regions which is higher than those for spectra peaks.

Organized Motions in the Velocity Field

The time-averaged velocity vectors in (x-z) plane are shown in Fig. 5. The visualized area with F105 lenz corresponds to x = 0 – 0.12 m and z = 0 – 0.12 m, which gives the ranges of normalized parameters, Grx' and z*, are from 2.6 × 10^5 to 3.0 × 10^8 (x'/D = 0.1 – 0.5) for x (x') in the horizontal direction, and from 0 to 245 in the vertical direction, respectively. The flow in the whole region is quite weak: the velocity is less than 0.4 ms^{-1}. The vectors show reasonable characteristics of flow fields qualitatively, e.g. suppression in vertical fluid motions due to wall effects near the upper surface, flow stagnation near the centre of heated round plate, activation of upward flow with z along the centreline due to the necking phenomena (Pham et al. 2007) and the entrainment of ambient fluid. The thickness of the boundary layer is about 50 zw.

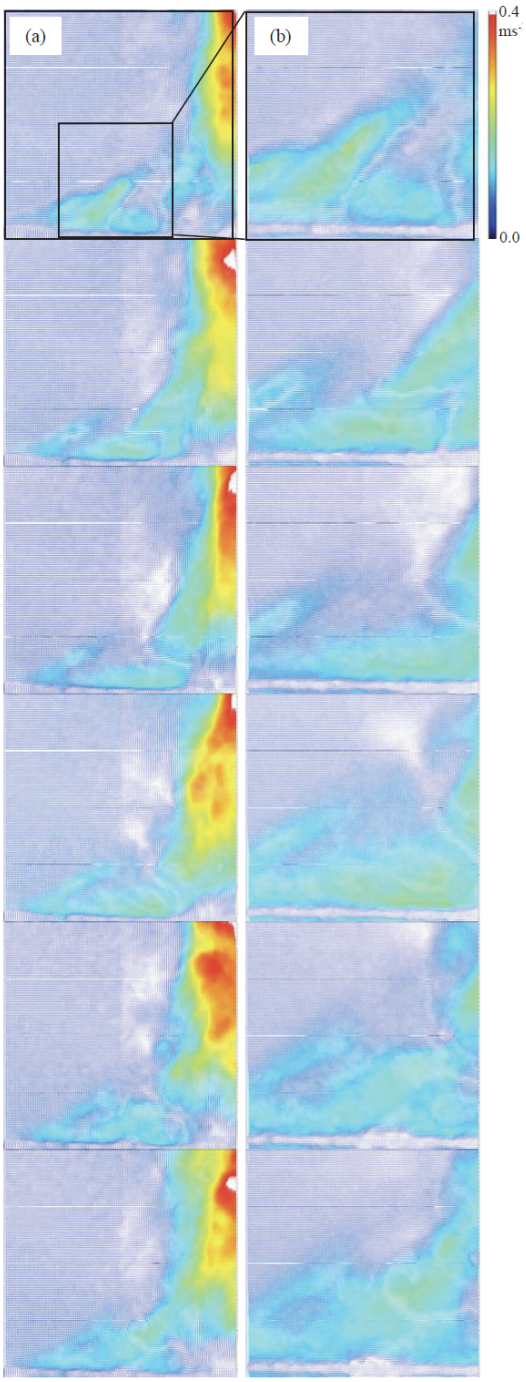

Figure 7. Example of time-series (from top to bottom) of reconstructed snapshot of velocity field with a F105 (a) and F200 (b) lenses, $\Delta\tau$ = 0.15 s.

The velocity fluctuation vectors with a F105 lens (x = 0 – 0.12 m and z = 0 – 0.12 m) for 4 most energetic POD modes are shown in Fig. 6. The contributions of these flow patterns to velocity fluctuations are quite large, i.e., the contributions of modes 1 – 4 are about 50%. Note that, the POD modes must be multiplied by its corresponding POD-coefficient to represent real vectors, and thus the sign and the length of the vectors do not have physical meaning until combined with the coefficients

used in reconstruction of snapshots. As shown in the figure, the flow pattern changes with POD modes, i.e., vectors of mode1 show lapping flows at the upper border of the boundary layer with cell structures in the vicinity of the heated surface, and the vectors of mode2 gives activations of the lapping flows and weaken the cell structures. These flow patterns occur in the almost whole visualized region, implying that the scale of flow field becomes quite large even in the near-surface region.

Figure 7 depicts an example of time-series (from top to bottom) of reconstructed snapshot of velocity field obtained by POD modes for data with a F105 (a) and F200 (b) lenses. Time-steps were set to 0.15 s to examine the dynamics of organized motions and temporal structures of the boundary layer. The boundary layer generates pseudo wavy structures with attenuations of lapping flows and activations of lower layer flows. Such structures yield changes in intensities of plume and also large-scale vortex motions intermittently.

SUMMARY AND DISCUSSION

In this study, a development processes, including turbulence transitions, of a natural-convection boundary layer in air along an isothermally heated round plate was experimentally investigated. Special attention was paid to the interaction with organized motions in a buoyant plume above the boundary layer. The values of dimensionless temperature difference and Rayleigh number based on the diameter were about 0.6 and 3.0×10^8, respectively, which correspond to those for a turbulent boundary layer above the heated plate with non-Boussinesq effects. The turbulence statistics of temperature fluctuations in the boundary layer, including near the heated surface, were measured by a cold wire, and 2-components velocity vectors in a vertical plane of the boundary layer and of the buoyant plume were measured by using a PIV measurement. The dynamic ranges of PIV measurement were improved by a two-camera PIV technique, and the accuracy of PIV measurement was verified through the comparison with a hot-wire measurement.

The critical Grashof number in the present study, $Gr_x' = 7.0 \times 10^6 - 1.7 \times 10^7$, estimated by increasing in the intensities of temperature fluctuations in the boundary layer agreed well with those obtained in previous studies (Kitamura and Kimura 1995, Kitamura and Kimura 2007). The profiles of the intensities of temperature fluctuations normalized with Townsend's (molecular) characteristics scales showed the similarity of thermal boundary layer generated above the heated surface, i.e. the normalized profiles of the present study agreed with those of Rayleigh-Benard convection under turbulence conditions (Theerthan and Arakeri, 1998). Notice that, the intensities before the transition were not necessarily zero, which implies that there exists some dynamics of boundary layer even near the edge of the heated surface.

The velocity fluctuation vectors for 4 most energetic POD modes, the contributions of which to velocity fluctuations were about 50%, showed the existence of the organized motions, lapping flows at the upper border of the boundary layer with cell structures in the vicinity of the heated surface. These flow patterns occur in the almost whole visualized region, implying that the scale of flow field becomes quite large even in the near-surface region. Also, time-series of reconstructed snapshot of velocity field obtained by POD modes revealed the boundary layer generates pseudo wavy structures with attenuations of lapping flows and activations of lower layer flows, and such structures yield changed in intensities of plume and also large-scale vortex motions intermittently. Namely, the coexistence of the development of boundary layer, which yields turbulence transitions with vortices intermittently moved toward the centre of the plate gives the unsteady evolution of the boundary layer with wavy motions and such the interaction between the organized motions and the boundary layer flow naturally yields the heat transfer processes with long characteristic time and length scales, which is much large compared with that of the boundary layer.

The authors would like to thank Mr. Takayoshi Mizuno for help in the experiments.

REFERENCES

Adrian RJ, 1996, "Variation of temperature and velocity fluctuations in turbulent thermal convection over horizontal surfaces,"Int J Heat Mass Transf 39, pp. 2303-2310.

Ai J, Law AW, Yu SCM, 2006, "On Boussinesq and non-Boussinesq starting forced plumes,"J Fluid Mech 558, pp. 357-386.

Brown E, Ahlers G, 2006, "Rotations and cessations of the large-scale circulation in turbulent Rayleigh-Benard convection," J Fluid Mech 568, pp. 351-386.

Hattori Y, Tsuji T, Nagano Y, Tanaka N, 2006, "Turbulence characteristics of natural-convection boundary layer in air along a vertical plate heated at high temperatures," Int J Heat Fluid Flow 27, pp. 445-455.

Hattori Y, Suto H, Nakao K, Hirakuchi H, 2018, "Insight into coherencew1 structure in logarithmic region of wall turbulence with detached eddy by using conditionally averaged two-camera PIV measurements," J Flow Vis Image Process 25, pp. 1-14.

Hu L, Hu J, de Ris JL, 2015, "Flame necking-in and instability characterization in small and medium pool fires with different lip heights," Combustion and Flame 162, pp. 1095-1104.

Khalifa A-J N, 2001, "Natural convection heat transfer coefficient – a review 1. Isolated vertical and horizontal surfaces," Energy Conv and Manag 42, pp. 491-504.

Kitamura K, Kimura F, 1995, "Heat transfer and fluid flow of natural convection adjacent to upward-facing horizontal plates," Int J Heat Mass Transf 38, pp. 3149-3159.

Kitamura K, Kimura F, 2007, "Fluid flow and heat transfer of natural convection over upward-facing horizontal heated circular disks," Trans JSME B73, pp. 2303-2310.

Theerthan SA, Arakeri JH, 1998, "A model for near-wall dynamics in turbulent Rayleigh-Benard convection," J Fluid Mech 373, pp. 221-254.

Tsuji T, Nagano N, Tagawa M, 1992, "Frequency response and instantaneous temperature profile of cold-wire sensors for fluid temperature fluctuation measurements," Exp Fluids 13, pp. 171-178.

Pham MV, Plourde F, Doan KS, 2007, "Direct and large-eddy simulations of a pure thermal plume," Phys Fluids 19, 125103.

Plourde F, Pham MV, Doan KS, Balachandar S, 2008, "Direct numerical simulations of a rapidly expanding thermal plume: structure and entrainment interaction," J Fluid Mech 604, pp. 99-123.

Watanabe R, Gono T, Yamagata T, Fujisawa N, 2015, "Three-dimensional flow structure in highly buoyant jet by scanning stereo PIV combined with POD analysis," Int J Heat Fluid Flow 52, pp. 98-110.